Carbonates Evaporites (2016) 31:139–151
DOI 10.1007/s13146-015-0249-2

ORIGINAL ARTICLE

Rare earth elements and stable isotope geochemistry of carbonates from the mélange zone of Manipur ophiolitic Complex, Indo-Myanmar Orogenic Belt, Northeast India

A. K. Singh[1] · V. C. Tewari[1] · A. N. Sial[2] · P. P. Khanna[1] · N. I. Singh[3]

Accepted: 15 May 2015 / Published online: 28 May 2015

Abstract Carbonates that occur in the mélange zone of Manipur ophiolitic complex (MOC), Indo-Myanmar Orogenic Belt, Northeast India contain diverse fauna with dominance of foraminifera assemblages (planktonic and benthic) and calcareous nanofossils. Rare earth element (REE) contents (~51 ppm average value) in the MOC carbonates are high compared with the average value of typical marine carbonate (~28 ppm). The Post-Archean Australian Shale (PAAS)-normalized REE patterns of these carbonates exhibit seawater-like REE patterns with light rare earth elements (LREE) depletion and relative heavy rare earth elements (HREE) enrichment with negative Ce anomalies (Ce/Ce* = 0.28–0.69) and positive Eu anomalies (Eu/Eu* = 1.07–2.08). The carbonates show depleted values of $\delta^{13}C$ ‰ (PDB) (0.89–2.74 ‰) which characterize marine precipitates while depletion in $\delta^{18}O$ ‰ (PDB), reaching minimum values (−6.29 to −11.40 ‰). The negative anomalies of Ce in these carbonates suggest that they were deposited under oxygenated environment. The observed shale-normalized positive Eu anomalies and spread in negative $\delta^{18}O$ values to a lesser extent of $\delta^{13}C$ ‰ (PDB) values of these carbonates suggest their formation were altered by diagenesis in shallow marine environment. Field, petrographical studies in conjunction with REE and stable isotope characteristics suggest that these carbonates form part of the ophiolitic mélange zone that emplaced during subduction and obduction processes of the Indian plate and Myanmar plate collision.

Keywords Carbonates · Rare earth element · Stable isotope · Ophiolitic mélange · India

Introduction

The carbon and oxygen isotopic compositions of carbonate rocks provide useful information on physico-chemical conditions of precipitation and its subsequent diagenesis, paleoclimate and paleoecology over geological times (James and Choquette 1984; Wright 1990; Madhavaraju et al. 2004; Tewari and Sial 2007). Because, the carbon isotopic composition in carbonate minerals are mainly identified by the $\delta^{13}C$ values of bi-carbonate/carbonate ions in the water, the $\delta^{18}O$ values are largely influenced by the isotopic composition of water and temperature of precipitation. Conversely, rare earth element (REE) concentrations in ancient carbonate rocks are useful to identify the marine versus non-marine sources of REE (Frimmel 2009; Zhao et al. 2009). REEs are also considered as an indicator to identify the depositional environmental system such as widespread marine anoxia (German and Elderfield 1990; Murray et al. 1991), oceanic palaeo-redox conditions (Elderfield and Pagett 1986; Kato et al. 2002), variations in surface productivity (Toyoda et al. 1990), proximity to source area (Murray et al. 1991), lithology and diagenesis (German and Elderfield 1990; Nath et al. 1992; Armstrong-Altrin et al. 2003, 2011; Madhavaraju et al. 2010) and paleogeography and depositional models (Kemp and Trueman 2003).

✉ A. K. Singh
aksingh_wihg@rediffmail.com

[1] Wadia Institute of Himalayan Geology, 33 GMS Road, Dehradun 248001, India

[2] NEG-LABISE, Department of Geology, University of Pernambuco, Recife 50732-970, Brazil

[3] Department of Geology, D. M. College of Science, Imphal 795138, India

The Nagaland–Manipur ophiolites (NMO) form part of the Tethyan ophiolites and occur in the NNE–SSW trending the IMOB, northeast India (Fig. 1a). The NMO occur as a narrow belt, ~200 km in length, ~2–20 km in width, covers an area ~2000 sq. km. It is represented by dismembered mafic–ultramafic rocks and podiform chromitites with closely associated oceanic sediments (cherts, cherty quartzite, greywake, phyllite, carbonate). Although the ophiolitic suite of rocks of the NMO has been the subject of intensive geological investigations (Ghose and Singh 1981; Chattopadhyay et al. 1983; Venkataramana et al. 1986; Mitra et al. 1986; Agrawal and Ghose 1986; Sengupta et al. 1989; Vidyadharan et al. 1989; Acharyya et al. 1989; Bhattacharjee 1991; Acharyya 2007; Chatterjee and Ghose 2009; Ghose et al. 2010; Singh et al. 2012; Singh 2009, 2013), the associated carbonates have received little attention (Acharyya et al. 1986; Mitra et al. 1986; Chungkham et al. 1992; Chungkham and Jafar 1998), and detailed geochemical data have not been investigated.

To address this gap in the data, this study reports on the carbon and oxygen stable isotope ratios along with REE contents of carbonate exotics (olistoliths) occurring in the southern part of the NMO, i.e. the Manipur ophiolitic Complex (MOC) of the Northeast India (Fig. 1b). These data are used to reconstruct the tectonic environment of the MOC carbonates deposition.

Geological setting

The Tethyan ophiolites exposed along curvilinear suture zones in the Alpine–Himalayan orogenic system are highly diverse in terms of their structural–petrological features and emplacement mechanisms (Dilek and Furnes 2009) (Fig. 1a). The ophiolite suite of rocks of the W–E trends Indus–Yarlung Tsangpo suture zone turning sharply southwestward at the eastern Himalayan syntaxis, is offset northward by the Sagaing fault, and continues southward along the Indo-Myanmar Orogenic Belt (IMOB) (Gansser 1980) (Fig. 1a). Further trends south to the Andaman–Nicobar Islands Arc and continues to southeast to the Mentawai Islands representing the outer Indonesian Island Arc.

The formation of the NMO is related to subduction and obduction processes caused by the collision of the Indian plate and the Myanmar plate (Acharyya et al. 1989; Mitchell 1993). The ophiolite sequence in this region is tectonised, dismembered and shows three phases of deformational events broadly comparable to the Himalayan orogeny and sea floor spreading of the Indian Ocean (Ghose et al. 1986). The ophiolites show an east-dipping thrust contact with the underlying Upper Cretaceous–Upper Eocene flysch-like sediments of the Disang and Barail formations exposed in the west, and are overthrusted from the east by continental metamorphic rocks such as quartz–mica schist, garnet–mica schist, quartzite, and granitic gneiss (Brunnschweiler 1966). It has been described that this ophiolite sequence was generated during the beginning of spreading of ocean basin, which escaped re-equilibration and significant fractionation developed at the edge of ocean basin adjacent to the continental margins (Vidyadharan et al. 1989). Acharyya et al. (1990) explained that this ophiolite is represented by dismembered mafic and ultramafic rocks with closely associated oceanic sediments and occurs as folded thrust slices occupying the highest tectonic levels that are brought to lie over distal shelf sediments of Eocene to Oligocene age. Singh et al. (2012) and Singh (2013) proposed that this ophiolite was initially formed in a mid-oceanic ridge tectonic setting and little modified by later subduction-related tectonic and petrological processes.

Stratigraphically, the investigated area (Fig. 1b) comprises of three major lithologic groups: ophiolitic suite, Disang group and Barail group. The ophiolitic suite of rocks consists of peridotites, basalt and gabbro with associated sediments of chert, conglomerate, carbonate and minor chromitites. The Disang group is exposed to west of ophiolites and consists of slate, graphitic slate, phyllite, siltstone and fine-grained sandstone. The ophiolitic suite of rocks are also intermixed and interbedded with the Disang flyschoid sediments (Bhattacharjee 1991). This group is subdivided into two formations as lower Disang and upper Disang formations. The Barail Group is made up of massive to thickly bedded sandstone, alternation of sandstone and shale. The Disang–Barail sequence, again, overthrust the Surma–Tipam Molasse belt towards west.

The olistoliths exposed as small lensoid exotic bodies in the mélange zone. These exotic bodies include carbonates, cherts, gritty sandstones and recrystallized sediments and are dispersed within the shale–siltstone–graywacke of the Disang group. Mitra et al. (1986) assigned the age of the NE–SW trending olistrostromal belt in the Nagaland ophiolite Complex (NOC) which is the northern part of the NMO of varying age ranging from Palaeocene to upper middle Eocene. Conversely, Chungkham and Jafar (1998) assigned the pelagic limestones (carbonates) of the MOC to the Late Cretaceous (Santonian–Maastrichtian), based on the integrated Coccolith–Globotruncanid biostratigraphy. Thus, age of the olistoliths of the NMO spans the interval of Late Cretaceous–palaeocene/Eocene. These ages are also similar to those microfaunal ages from cherts and limestones from the NMO reported by Ghose et al. (1984). Thus, there is general agreement that the upper limit age of NMO probably extends up to Eocene while the lower age limit is probably Late Cretaceous. Recently, Baxter et al. (2011) reported Upper Jurassic radiolarians cherts collected from the NMO. This new age is also supported by earlier

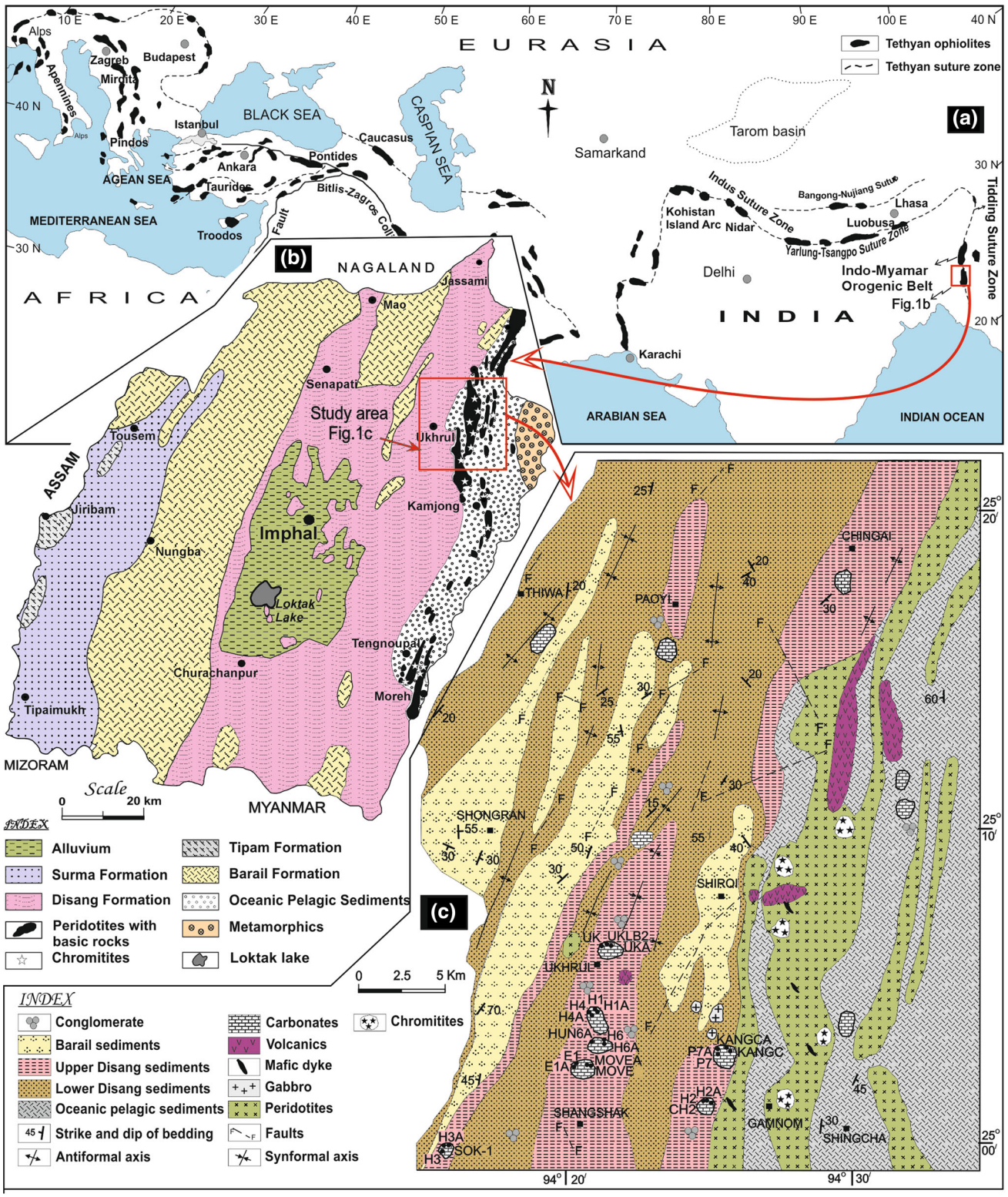

Fig. 1 **a** Map of the major Tethyan ophiolites and suture zones in the Alpine–Himalayan System (after Dilek and Furnes 2009). **b** Generalized geological map of Manipur, Northeast India (after GSI, M.N.C. DRG. No. 42/87, 1987), showing the Manipur ophiolitic Complex (MOC), Indo-Myanmar Orogenic Belt, Northeast India. **c** Geological map of the study area in the MOC, Northeast India (after Singh et al. 2012)

single radiometric age of 148 ± 4 Ma (whole rock K–Ar) from an associated basaltic flow with cherts in the NOC (Sarkar et al. 1996). Conversely, Bhattacharjee (1991), based on radiolarian fossils (Nassellaria), assigned the age of the MOC chert as Early to Middle Cretaceous. Consequently, the original age of the rocks forming the NMO is still controversial.

Facies of different carbonate olistoliths

The investigated carbonates in general are fine grained and show various shades of colour ranging from white, grey, buff and brown. Minor amount of disseminated pyrite, veins of calcite and quartz, along with irregular stylolitic and stalactitic structures are also observed in these carbonates. In Ukhrul area, carbonate deposits are located at about 400 m east of viewland market, Ukhrul town (Fig. 2a) and near the Ukhrul–Jessami road. They are white and buff in colour and exhibit tectonic contact with the Disang formation. There are three carbonate deposits in Hundung area, i.e. north deposit (Fig. 2b), the Mova cave deposit and Hundung south deposit. Megascopically, carbonates of Hundung area show white to shades of grey, buff and pink colours. These carbonates are fine grained and exhibit subconchoidal fracture. At places, the carbonates show irregular stylolitic structures and intercalated with grey shale. The Kangkhui carbonate deposits are located near Kangkhui village, about 13 km from Ukhrul town (Fig. 2c). They are white and light pink in colour, massive and highly jointed. These carbonates occur in pyramidal/conical form associated with Disang shale. The other minor carbonate deposits are Sokpao and Changa deposits (Fig. 2d). Carbonates in Sokpao are white, massive and show subconchoidal fractures. In Changa area, carbonates are grey in colour and show vein with subconchoidal fractures. They are characterized by the presence of aggregate-type stylolitic veins and minute fractures exhibiting fine laminations (Fig. 2e).

Petrographic studies of these carbonates confirmed that they are mainly composed of calcite with minor amount of dolomite, quartz and clay minerals with larger and smaller microfossils. Sparse biomicrite or biomicrite is the dominant microfacies in which allochems are either embedded

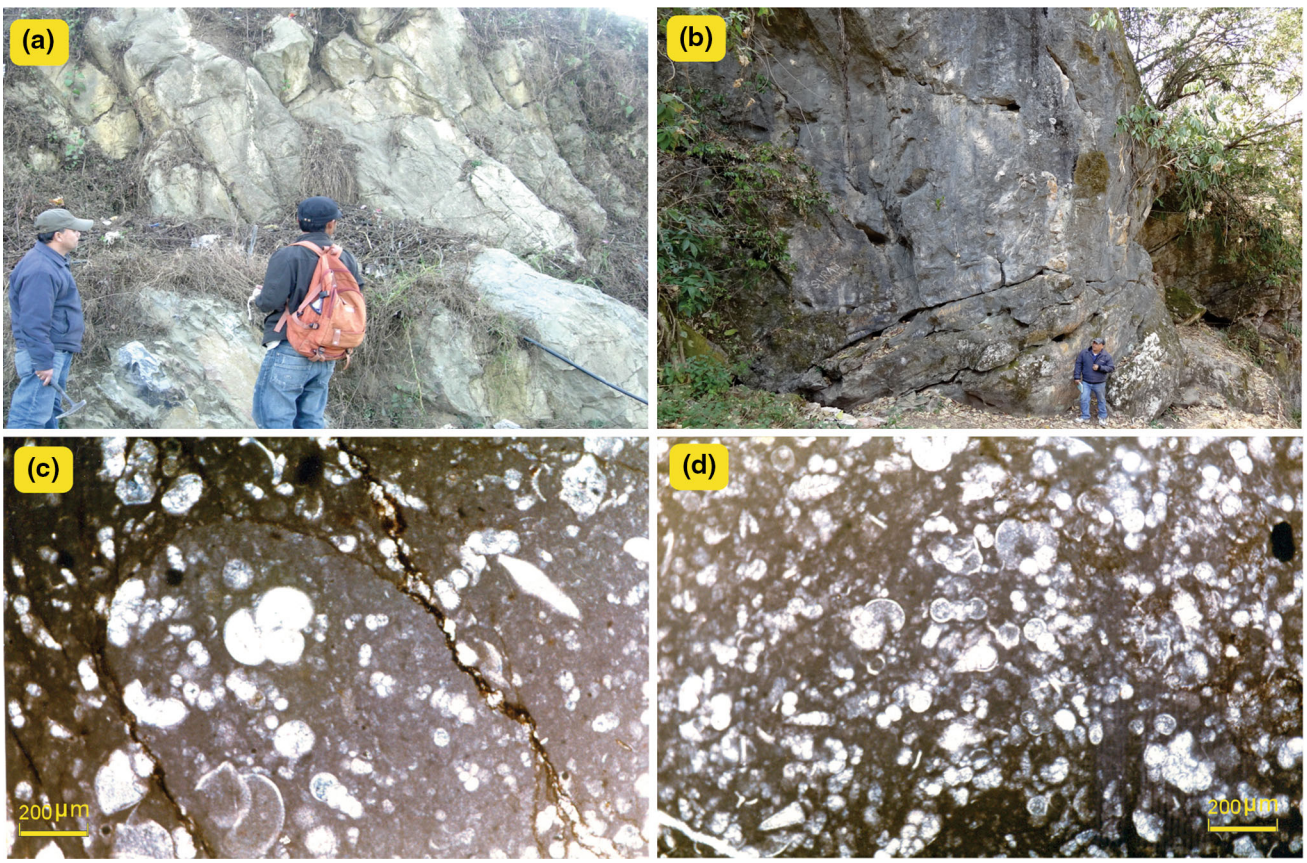

Fig. 2 Field photographs of selected carbonate deposits in the study area **a** Bedded carbonate deposit near Ukhrul viewland bazaar; **b** Kangkhui carbonate deposit. Photomicrographs **c** showing stylolitic structure filled with ferrugineous matrix in the sparse biomicrite of carbonate from Khangkhui area **d** showing packed biomicrite carbonate from Hundung area

in the groundmass of calcite matrix or are cemented by calcite matrix (Fig. 2f). Majority of the carbonate grains, in the present case, are <0.004 mm in size. Some grains are rounded and have reached up to 0.01 mm.

The carbonates in Ukhrul are very fine grained. Fractured veins are filled with calcite, quartz, kaolinised feldspar. The stylolites aggregate types are filled with argillaceous/ferruginous matter. The observed amount of allochem (10–50 %) classifies the rock as sparse biomicrite (Folk 1962). The Hundung carbonates are homogenous and dense sub-translucent in thin sections. Presences of macrostylolites are noticed in few thin sections. There are three types of carbonates that have been identified as sparse biomicrite, packed biomicrite and fossiliferous micrite (Folk 1962). Grains in these carbonates are very fine, average size ranging from 0.001 to 0.003 mm but some of them reach up to 0.006 mm. The inequigranular grains of the carbonates are anhedral to subhedral. The Kangkhui carbonates comprise very fine grains ranging in size from 0.002 to 0.004 mm. Xenotopic to hypidiotopic fabrics are observed in the Kangkhui carbonates. The fractures are filled with sparry calcite, minor dolomite, quartz and kaolinised feldspar. These carbonates are identified as fossiliferous micrite as the allochem constitutes less than 10 % (Folk 1962). In the Changa carbonates microfracture veins are irregular and are filled with calcite spars and siliceous materials. These carbonates are also identified as fossiliferous micrite. Sokpao carbonates show xenotopic to hypidiotopic fabric and they have very less allochems. The important allochems are the fragments of macrofossils and pellets.

The studied carbonates yield diverse microfossil assemblages comprising planktonic and benthic foraminifera and also calcareous nanofossils. Integrated biostratigraphy of these carbonates is documented in Chungkham et al. (1992) and Chungkham and Jafar (1998).

Analytical methodology

X-ray powder diffraction (XRD) analyses of seven representative samples were carried out at the Wadia Institute of Himalayan Geology (WIHG), Dehradun. Powder XRD patterns were collected using a PANalytical, X'pert PRO X-ray Diffractometer at room temperature, using a rotating Cu target with a voltage of 45 kV and a current of 40 mA. The scan range (2θ) was 2°–60° with a step size of 0.0080°.

Rare earth element (REE) concentrations of the representative carbonate samples were analysed by inductively coupled mass spectrometry (ICP-MS, ELAN DRC-E, Perkin Elmer) at analytical accuracy ranges from 2 to 12 % and precision varies between 1 and 8 %. REE concentrations of carbonates are presented in Table 1. Their average REE ratios are compared with the values of shallow and deep water marine carbonate sediments presented in Table 2.

Carbon and oxygen isotope analyses were carried out at the Stable Isotope Laboratory (LABISE) of the Federal University of Pernambuco, Brazil. Few samples (UKLB, HUN-6A, KANG-CA, MOVA-EA, SOK-1, CH-2) were analysed at the isotope laboratory of the ONGC, Dehradun. The results are reported as permil (‰) $\delta^{18}O$ and $\delta^{13}C$ values relative to Pee Dee belemnite (PDB). The conversion of SMOW (Standard Mean Ocean Water) values to PDB standard have been attempted using the following formula $\delta^{18}O$ calcite (SMOW) = 1.03086 $\delta^{18}O$ calcite (PDB) = 30.86 (Friedman and O'Neil 1977). The carbon and oxygen isotopic data of the twenty four representative samples are presented in Table 3.

Results and discussion

X-ray diffraction analysis

The X-ray diffractograms of representative MOC carbonate samples (UK, H1, H6, P7A, E1, H3, H2) are reported in Fig. 3. The peaks are quite sharp with little background absorption. It revealed that it contains calcite as the major mineral phase while quartz as the minor silicate gangue mineral in all the carbonate samples.

Rare earth elemental characteristics

The total REE (ΣREE) contents of the MOC carbonates range from 13.49 to 81.94 ppm, with an average of 51 ppm (Table 1). Significant variations in ΣREE content are noticed in the different types of carbonates. The carbonate samples from the Hundung north have highest concentration (72.16–81.94 ppm) of ΣREE whereas the carbonates from Kangkhui have lowest ΣREE content (13.49–37.77 ppm). The low ΣREE in the Khangkui limestone is probably due to marine carbonate phases, which generally contain significantly lower REE content than detrital clays and heavy minerals (Palmer 1985).

Post-Archean Australian Shale (PAAS)-normalized REE patterns of these carbonates are shown in Fig. 4a. These carbonates exhibit seawater-like REE pattern with LREE depletion [average $(Nd/Yb)_{SN\ (shale\ normalized)} = 0.98 \pm 0.25$] and consistent negative Ce_{SN} and positive La_{SN} anomalies. The carbonate minerals precipitated in equilibrium with seawater show distinct negative Ce anomalies and this may also be reflected in the bulk REE pattern (Palmer 1985).

The $(Dy/Yb)_{SN}$ ratio in the MOC carbonates vary from 0.87 to 1.53 (average 1.28 ± 0.19), which is similar to the modern seawater (~0.8–1.1). The high $(Dy/Yb)_{SN}$ ratios in

Table 1 Representative rare earth element (REE) concentrations (ppm) in carbonates from the ophiolitic mélange zone of Manipur, Northeast India and Post-Archean Australian average shale (PAAS)

Sample location	Ukhrul proper			Hundung north			Hundung south			Kangkhui		Mova		Sokpao		Changa		Post-Archean Australian Shale
Sample	UK	UKA	UKLB	H1	H1A	H4	H5	H6	H6A	P7	P7A	E1	E1A	H3	H3A	H2	H2A	PAAS
La	11.53	9.10	9.90	18.46	20.40	17.50	12.40	13.43	13.90	12.20	4.22	13.06	12.30	17.24	18.00	11.83	13.20	38.20
Ce	12.35	13.20	14.00	22.15	23.60	23.60	14.60	9.76	10.90	6.60	2.56	10.16	9.30	16.71	17.30	12.49	13.80	79.60
Pr	2.56	1.80	2.00	4.39	4.30	3.30	2.70	2.51	2.60	1.90	0.65	1.98	1.90	3.29	3.50	2.77	2.70	8.83
Nd	10.42	8.20	8.80	16.56	18.80	14.70	13.30	11.41	11.80	8.40	2.90	8.94	9.20	14.08	14.80	10.62	12.00	33.90
Sm	2.11	1.64	1.71	3.35	3.56	3.02	2.66	2.70	2.33	1.61	0.56	2.59	1.55	3.23	2.88	2.06	2.46	5.55
Eu	0.47	0.44	0.46	0.79	0.82	0.80	0.67	0.77	0.58	0.41	0.15	0.95	0.48	0.91	0.68	0.49	0.57	1.08
Gd	2.00	1.24	1.35	3.25	2.86	2.39	2.31	2.19	2.05	1.54	0.57	1.78	1.49	2.41	2.39	2.19	1.99	4.66
Tb	0.30	0.25	0.25	0.47	0.55	0.49	0.46	0.40	0.41	0.31	0.10	0.33	0.30	0.45	0.47	0.31	0.39	0.77
Dy	1.42	1.23	1.35	2.64	3.07	2.63	2.47	2.49	2.37	1.90	0.66	2.17	1.92	2.60	2.59	1.87	2.16	4.68
Ho	0.34	0.25	0.26	0.51	0.60	0.57	0.51	0.54	0.50	0.43	0.15	0.54	0.46	0.56	0.52	0.37	0.44	0.99
Er	0.90	0.69	0.73	1.40	1.69	1.58	1.40	1.57	1.45	1.21	0.47	1.73	1.43	1.65	1.45	0.93	1.18	2.85
Tm	0.13	0.10	0.10	0.20	0.24	0.23	0.20	0.22	0.21	0.18	0.06	0.25	0.22	0.22	0.21	0.14	0.17	0.41
Yb	0.79	0.50	0.55	1.26	1.27	1.18	0.99	1.23	1.07	0.94	0.38	1.50	1.18	1.25	1.08	0.82	0.85	2.82
Lu	0.10	0.07	0.08	0.18	0.18	0.17	0.14	0.19	0.16	0.14	0.06	0.24	0.18	0.20	0.16	0.12	0.12	0.43
∑REE	45.42	38.71	41.54	75.60	81.94	72.16	54.81	49.41	50.33	37.77	13.49	46.22	41.91	64.80	66.03	47.01	52.03	175.94
$(La/Yb)_{SN}$	1.077	1.344	1.329	1.082	1.186	1.095	0.925	0.806	0.959	0.958	0.820	0.643	0.770	1.018	1.230	1.064	1.146	–
$(La/Nd)_{SN}$	0.982	0.985	0.998	0.989	0.963	1.056	0.827	1.045	1.045	1.289	1.291	1.296	1.186	1.087	1.079	0.989	0.976	–
$(Nd/Yb)_{SN}$	1.097	1.364	1.331	1.093	1.231	1.036	1.118	0.772	0.917	0.743	0.635	0.496	0.649	0.937	1.140	1.076	1.174	–
$(Dy/Yb)_{SN}$	1.083	1.482	1.479	1.261	1.457	1.343	1.503	1.220	1.335	1.218	1.047	0.872	0.980	1.253	1.445	1.370	1.531	–
Er/Nd	0.086	0.084	0.083	0.084	0.090	0.107	0.105	0.138	0.123	0.144	0.162	0.194	0.155	0.117	0.098	0.087	0.098	–
Eu/Eu*	1.077	1.453	1.426	1.132	1.210	1.402	1.273	1.491	1.250	1.226	1.250	2.083	1.487	1.536	1.220	1.084	1.213	–
Ce/Ce*	0.511	0.693	0.678	0.574	0.548	0.659	0.528	0.354	0.382	0.281	0.315	0.404	0.383	0.478	0.473	0.505	0.498	–
Pr/Pr*	1.254	1.000	1.040	1.296	1.144	1.024	1.062	1.237	1.214	1.301	1.250	1.148	1.109	1.193	1.212	1.335	1.160	–

Table 2 Average REE ratios of carbonates from the ophiolitic mélange zone of Manipur, Northeast India compared with the values of shallow and deep water marine carbonate sediments

Elemental ratios	Seawater[a]	Shallow marine carbonate, Late Cretaceous[b]	Shallow marine plateform carbonate Late Neoproterozoic[c]	Arabian sea carbonate sediments[d]	Indian ocean carbonate sediments[e]	Limestone from the present study
$(La/Yb)_{SN}$	0.2–0.5	1.82 ± 0.46	0.68 ± 0.47	0.85 ± 0.2	0.166 ± 0.953	1.02 ± 0.19
$(La/Nd)_{SN}$	0.8–2.0	1.22 ± 0.26	1.01 ± 0.20	0.98 ± 0.03	1.04 ± 0.19	1.06 ± 0.13
$(Nd/Yb)_{SN}$	0.20–0.49	1.51 ± 0.30	0.65 ± 0.39	0.85 ± 0.17	0.83 ± 0.13	0.98 ± 0.25
$(Dy/Yb)_{SN}$	0.8–1.1	1.25 ± 0.17	1.10 ± 0.25	1.12 ± 0.11	1.37 ± 0.05	1.28 ± 0.19
Er/Nd	0.27	0.07 ± 0.02	0.25 ± 0.17	0.11 ± 0.02	–	0.11 ± 0.03
Eu/Eu*	–	0.58 ± 0.11	–	1.15 ± 0.08	>1	1.34 ± 0.23
(Ce/Ce*)	<0.1–0.4	0.76–0.16	–	0.84 ± 0.06	0.30–0.84 Avg 0.56	0.48 ± 0.12
∑REE	–	73 ± 20	3.36 ± 2.55	78 ± 40	–	51.71 ± 16.60

[a] Data compiled by Nagarajan et al. (2011); [b] Madhavaraju and Ramasamy (1999); [c] Mazumdar et al. (2003); [d] Nath et al. (1997); [e] Nath et al. (1992)

Table 3 Carbon and oxygen isotope ratios for carbonates of the ophiolitic mélange zone of Manipur, Northeast India

Location	Sample no.	$\delta^{13}C$ ‰ (PDB)	$\delta^{18}O$ ‰ (PDB)	$\delta^{18}O$ ‰ (SMOW)	*Z* value
Ukhrul proper	UK	1.26	−7.31	23.33	126.24
	UKA	1.36	−7.21	23.43	126.49
	UKLB2	0.89	−8.50	22.00	124.89
Hundung north	H1	1.90	−6.68	24.18	127.86
	H1A	1.89	−6.68	24.18	127.84
	H4	1.33	−7.18	23.68	126.45
	H4A	1.53	−7.12	23.52	126.89
Hundung south	H6	1.61	−7.31	23.33	126.96
	H6A	1.59	−7.09	23.55	127.03
	HUN-6A	2.74	−8.50	22.00	128.68
Kangkhui	P7	1.93	−6.55	24.11	127.99
	P7A	1.98	−6.73	23.92	128.00
	KANK-C	1.67	−11.40	19.00	125.04
	KANG-CA	2.10	−10.50	19.10	126.37
Mova	E1	1.07	−11.35	19.16	123.84
	E1A	1.30	−8.89	21.69	125.54
	MOV-EA	1.39	−9.85	20.60	125.24
	MOV-E	1.59	−9.80	20.70	125.68
Sokpao	H3	2.09	−6.55	24.11	128.32
	H3A	2.10	−6.29	24.38	128.47
	SOK1	1.59	−9.80	20.70	125.68
Changa	CH2	1.52	−10.10	20.40	125.38
	H2	1.71	−7.08	23.78	127.28
	H2A	1.72	−6.97	23.89	127.35

Manipur carbonates show an enrichment in HREE rather than LREE, similar to modern seawater. La_{SN} and Ce_{SN} anomalies were calculated using the technique of Bau and Dulski (1996) (modified after Webb and Kamber 2000). In the PAAS-normalized Pr/Pr* $[Pr/(0.5Ce + 0.5Nd)]_{SN}$ vs. Ce/Ce* $(3Ce/(2La + Nd)_{SN}$ plot (Fig. 4b) all carbonate samples cluster in the field of negative Ce and positive La anomalies in agreement with modern open oceanic surface water.

The effects of LREE/HREE fractionation in modern and ancient marine systems can be represented by the Er/Nd ratio (German and Elderfield 1989). The high Er/Nd ratio

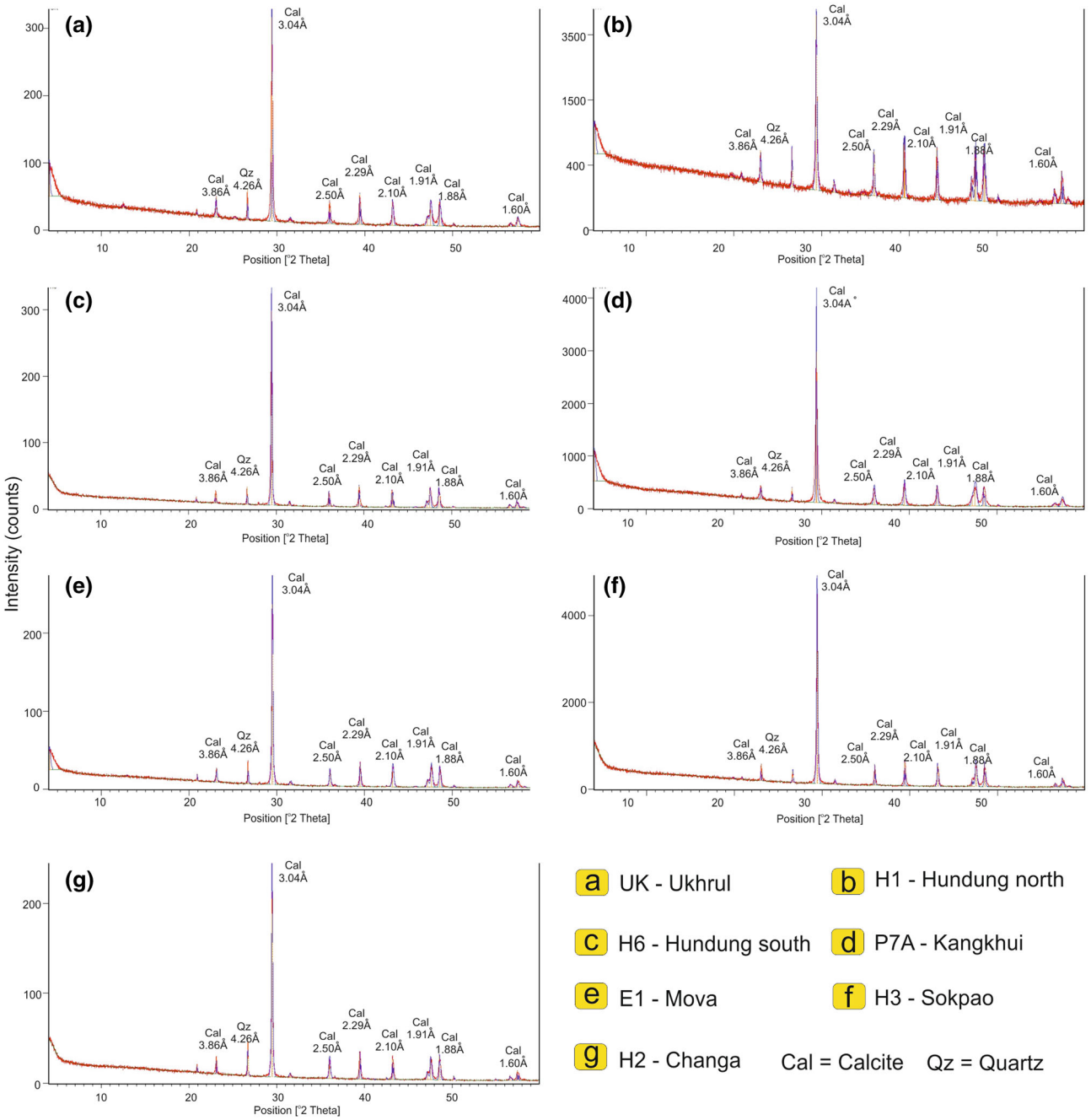

Fig. 3 X-ray diffractogram of representative samples of carbonate of the MOC, Northeast India

of carbonates effectively reveals the seawater signature retained by the marine carbonate. Er/Nd ratio in normal seawater is about 0.27 (De Baar et al. 1988). The addition of detrital material or diagenesis can reduce the Er/Nd value to <0.1 due to preferential concentration of Nd relative to Er (German and Elderfield 1989; Bellanca et al. 1997). The Er/Nd ratio of the MOC carbonates is ranging from 0.083 to 0.194 which indicates the influence of detrital materials in these carbonates (Table 1). The shale-normalized positive Eu anomalies (Eu/Eu*) are found either in waters affected by eolian input (Elderfield 1988) via river, hydrothermal solutions, and the sediments resulting from high T-basalt alteration along mid-ocean ridges, back arc spreading centre (German et al. 1993; Siby et al. 2008), and diagenesis (Murray et al. 1991) or variations in plagioclase content (Nath et al. 1992; Madhavaraju and Lee 2009). Positive Eu anomalies are uncommon in seawater, which generally result by input from hydrothermal

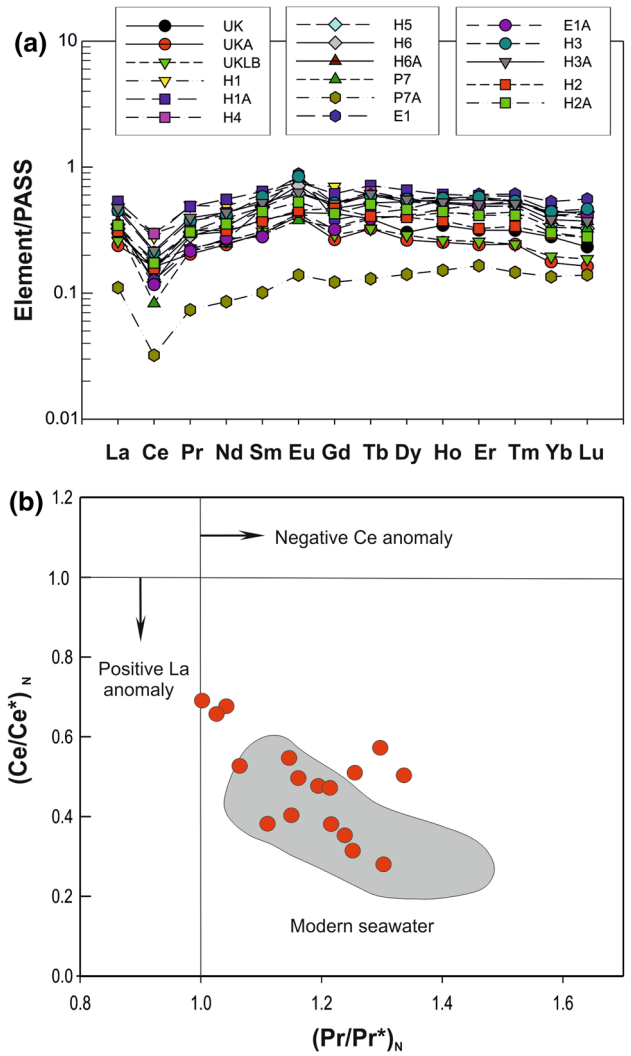

Fig. 4 **a** Post-Archean Australian Shale (PAAS) normalized REE patterns of carbonates from the Manipur ophiolitic mélange zone, Northeast India. **b** Plot of PAAS-normalized Pr/Pr* [Pr/(0.5Ce + 0.5Nd)]$_{SN}$ versus Ce/Ce* (3Ce/(2La + Nd)$_{SN}$ (after Bau and Dulski 1996; Webb and Kamber 2000). The plot discriminates between La and Ce anomalies, both may be present in seawater. All carbonate samples cluster in the field of negative Ce and positive La anomalies in perfect agreement with modern open oceanic surface water. The field of modern seawater is shown for comparison (after Nagarajan et al. 2011)

discharges along mid-ocean ridges (Klinkhammer et al. 1994). Positive Eu anomalies have been extensively well documented for hydrothermal vent fluids and sediment particulates in active ridge system (Douville et al. 1999; German et al. 1999). Derry and Jacobsen (1990) and Danielson et al. (1992) also proved that the marine positive Eu anomaly is caused by an increased oceanic input of hydrothermally originated fluids at mid-oceanic ridges. The studied MOC carbonates have large variations in Eu anomaly (Eu/Eu*), which range from 1.07 to 2.08 and display positive Eu anomalies. These positive Eu anomalies which is unusual in seawater probably resulted by the diagenetic alteration in the carbonate (Brand and Veizer 1980); a slight increase in the primary or detrital feldspar component (Madhavaraju et al. 2010) and an increased oceanic input of hydrothermally originated fluids at mid-oceanic ridges (German et al. 1999).

Carbon and oxygen isotopic variations

The stable carbon isotope composition ($\delta^{13}C$) reflects the source of CO_2 for precipitation, such as meteoric or sea water, shell dissolution, or various biochemical origins, including microbial oxidation of organic matter and methane whereas the stable oxygen isotope composition ($\delta^{18}O$) of a precipitated carbonate depends mainly on the isotope composition, salinity and temperature of the host fluid (Rankamma 1963; Friedman and O'Neil 1977; Leeder 1982). The negative oxygen isotope values reveal either to increased temperature or introduction of meteoric water during diagenesis, while the carbon fluctuations relate to presence of organic matter or CO_2 produced by various organic reactions (Armstrong-Altrin et al. 2009). Diagenesis often leads to more negative $\delta^{18}O$ values in marine carbonates (Land 1970; Allan and Matthews 1977), because cementation and recrystallization often take place in fluids depleted in $\delta^{18}O$ with respect to seawater (e.g. meteoric water) or at elevated temperatures (burial conditions).

The MOC carbonates show variable oxygen and carbon isotope data ranging for $\delta^{18}O$ from −6.29 to −11.40 ‰ (PDB) whereas $\delta^{13}C$ ‰ (PDB) ranges from 0.89 to 2.74 ‰ (PDB). To discriminate marine and freshwater carbonates the following equation proposed by Keith and Weber (1964), $Z = a(\delta^{13}C + 50) + b(\delta^{18}O + 50)$ in which 'a' and 'b' are 2.048 and 0.498 is employed. The carbonates with Z values above 120 are considered as marine, whereas those with Z values below 120 would be classified as freshwater type. Furthermore, the Z values are <120 for all the cement samples and come under the freshwater type. In the present study (whole rock samples), all the samples show Z values above 120 ranging from 123.84 to 128.68, indicating their marine origin (Table 3). The $\delta^{13}C$ ‰ (PDB) and $\delta^{18}O$ ‰ (PDB) ratios of these carbonates are closely similar to marine limestone (Fig. 5a).

The $\delta^{18}O$ versus $\delta^{13}C$ bivariate diagram with generalized isotopic fields for carbonate components, sediments, limestones, cements, dolomites, and concretions was first proposed by Hudson (1977). Later, Nelson and Smith (1996) modified and distinguished a number of characteristic isotope fields for carbonates of different origins. In this bivariate diagram (Fig. 5b) most of the MOC carbonates plot in the marine limestone and burial cements field, which also reveals the alteration during diagenesis.

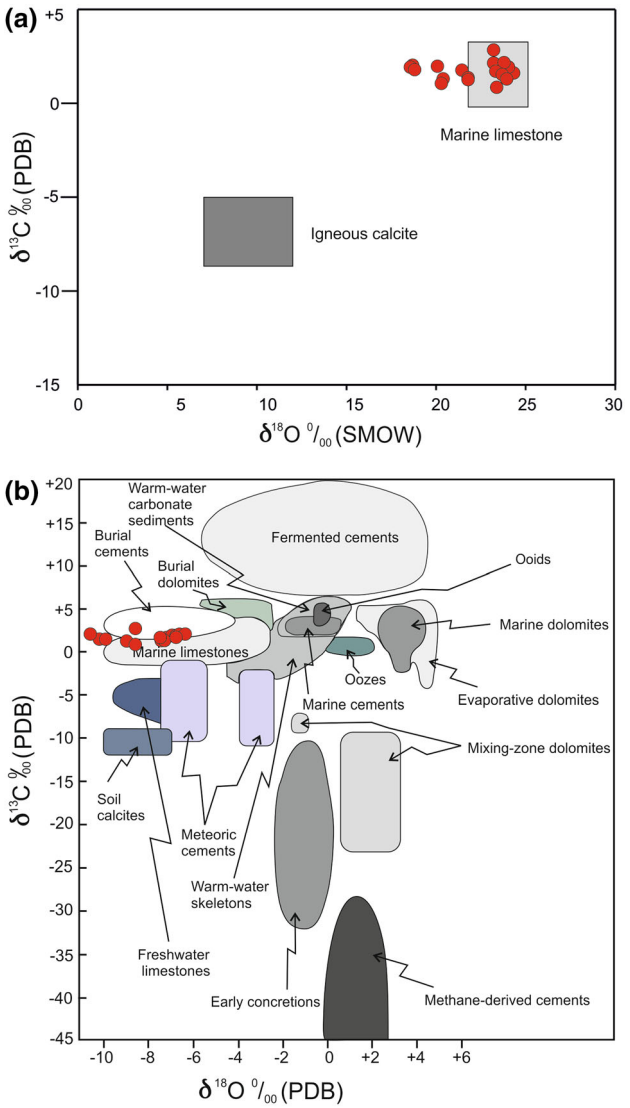

Fig. 5 **a** Bivariate plots of $\delta^{18}C$ (SMOW) and $\delta^{13}O$ (PDB) and **b** $\delta^{18}C$ (PDB) and $\delta^{13}O$ (PDB) plot for carbonates the Manipur ophiolitic mélange zone, Northeast India. Fields in **a** are after Bowman (1998) and in **b** are after Hudson (1977), Nelson and Smith (1996)

Tectonic environment of the MOC carbonate deposit

Differences in ΣREE content among the individual samples are mainly due to variations in the amount of terrigenous sediment included in these carbonates. The average REE concentration of the MOC carbonates (ΣREE = 51.71 ± 16.60 ppm) is more or less comparable with the shallow marine carbonates of Maastrichtian limestones (ΣREE = 73 ± 20). However, they are higher than the typical marine carbonate value (~28 ppm, Bellanca et al. 1997) and the shallow marine continental platform carbonates of Late Neoproterozoic (ΣREE = 3.36 ± 2.55 ppm, Mazumdar et al. 2003). REEs (La to Lu) show positive inter-elemental relationships, indicating their coherent nature, which reveal that they are highly linked with seawater during the REE fractionation. The extent of Ce depletion reflects oxygenation state of the water (Komiya et al. 2008; Zhao et al. 2009). The negative anomalies of Ce in these carbonates suggest that they were deposited under oxygenated environment. In addition, there is no remarkable variation in Ce anomalies in these carbonates which suggests that there were not much fluctuation in bottom water oxygen level. The $\delta^{13}C$ values show statistically positive correlation with $\delta^{18}O$ values, such positive relationship between $\delta^{13}C$ and $\delta^{18}O$ indicates that these carbonates were altered by diagenesis (Buonocunto et al. 2002). Diagenesis often results in more negative $\delta^{18}O$ values in marine carbonates (Allan and Matthews 1977), because cementation and recrystallisation often take place in fluids depleted in $\delta^{18}O$ with respect to sea water or at elevated temperatures. Hence, the observed spread in negative $\delta^{18}O$ values of the MOC carbonates indicates that they were altered by diagenesis.

Considering the REE and stable isotope characteristics of these investigated carbonates, it is likely that the MOC carbonates were influenced by diagenetic activities at different tectonic processes during the evolution of Nagaland–Manipur ophiolites. The following discussion briefly explains the record of tectonic environment of the MOC carbonates deposition.

The ophiolitic mélange in the study area is a disorganized association of various tectonic slivers of Late Cretaceous to Eocene age, has been inferred to be an accreted terrain deformed in a convergent trench setting. The W–E trending Indus–Yarlung Tsangpo suture zone (IYSZ) includes ophiolitic mélange, turbidites, calc alkaline volcanics, batholith and post-orogenic sedimentary deposits (Upadhyay and Sinha 1998). The IYSZ swerves sharply southwestward at the eastern Himalayan syntaxis at Namche Barwa and are offset northward by the Sagaing fault, and continue southward along the IMOB (Fig. 1a) (Gansser 1980; Acharyya et al. 1989; Mitchell 1993; Searle et al. 2007). It further extends south to the Andaman–Nicobar Islands Arc and continues to southeast to the Mentawai Islands representing the outer Indonesian Island Arc. The NMO form a part of the Tethyan ophiolite belt exposed in the NNE–SSW trending IMOB (Fig. 1a). The NMO have been interpreted as an accretion prism resulting from the convergence between the Indian and Myanmar plates (Acharyya et al. 1989; Mitchell 1993). The facies distribution in the IMOB indicates that the basin was differentiated in Upper Cretaceous time itself into a shallow shelf basin in Assam (up to Shillong plateau) and a deeper geosynclinal part in the IMOB (Ghose et al. 1986). In the eastern side, the basin was deeper with a pelagic facies

(radiolarian chert, limestone, greywake, shale and phyllite) with intermittent basaltic flows followed by a trench with flysch facies of Disang formation along the IMOB. It has been reported that the initial rifting and creation of the Indo-Myanmar Ocean took place prior to Latest Santonian/Early Campanian period (Chungkham and Jafar 1998). At this oceanic crust formation stage in a mid-oceanic ridge tectonic regime, plutonic and volcanic activity took place. As a result of the separation of the melt that formed through low-degree partial melting of the upper mantle, less depleted lherzolite and slightly depleted cpx-harzburgite are left over and (Singh 2013). Ultramafic rocks from the oceanic crust as well as from the upper mantle moved up along with the formation of the ridges. Mafic rocks and sediments were also raised up in the ridges. Later, the entire platform was covered by pelagic sediments.

By the end of the extensional tectonic regime and the initiation of ocean closure, the eastern oceanic part of the Indian plate started to subduct eastwards under the Myanmar plate. This eastward subduction of the Indian plate beneath the Myanmar plate leading to the Late Cretaceous to Early Paleogenic crust was accreted in a trench/forearc setting. Topographic peaks of the accretionary complexes, i.e. trench–slope breaks, reached close to or above sea level, and strata containing carbonate bodies appear to have formed either on the shallower coastal slopes or on the gently raised platform produced by slow uplift of the pelagic sediments. Fragmented shallow marine rock bodies including carbonates were transported into deeper depositional environments, such as trench–slope basins, by gravity flows and submarine slides. Radiolarian cherts were deposited within deep ocean floor below the carbon compensation depth. The age of radiolarian cherts indicates that the development of a trench along the western margin of the Myanmar plate took place during middle Cretaceous (Bhattacharjee 1991). In the western part of the trench, on the Indian land mass, the fyschoid Disang Formation was deposited, simultaneously with deposition of radiolarian cherts in the trench and carbonates on elevations of the floor of the basin. Some of these materials were exhumed and recycled as multiple debris flows during Late Cretaceous–Eocene. The subsequence geological processes including climatic and oceanographic changes lead to form ophiolitic melange zone of the MOC that include partially or totally serpentinized peridotites, gabbro, diabase, basalt, pelagic sediments and olistoliths. In the later part of Early Eocene, the subduction rate decreased at the suture due to the entry of a sea-mount into the subduction zone (Acharyya 2007). Later, the IMOB became stable and the MOC exposed in the eastern flank of the IMOB.

Conclusions

The Phanerozoic Nagaland–Manipur ophiolites (NMO) are a part of the Indo-Myanmar Orogenic Belt (IMOB), northeastern India. The NMO are represented by dismembered mafic–ultramafic rocks and podiform chromitites with closely associated oceanic sediments (cherts, cherty quartzite, greywake, phyllite, carbonate). Carbonates that occur in the ophiolitic mélange zone of Manipur ophiolite complex contain diverse fauna with dominance of foraminifera assemblages (planktonic and benthic) and calcareous nanofossils. As a whole, in the studied carbonates, sparse biomicrite or biomicrite is the dominant microfacies in which the fossil allochems are embedded in the groundmass of calcite matrix or the fossil allochems are cemented by calcite matrix which is indicative of low-energy environment. These carbonates show variable contents of REE range from 13.49 to 81.94 ppm and an average of 51 ppm which is higher than the average value of typical marine carbonate ($\sim$28 ppm). The increase in negative $\delta^{18}O$ with that of positive $\delta^{13}C$ values may reflect either increasing temperature or influx of meteoric water. The observed shale-normalized positive Eu anomalies, negative Ce anomalies and spread in negative $\delta^{18}O$ ‰ (PDB) to a lesser extent of $\delta^{13}C$ ‰ (PDB) values of these carbonates suggest that their formation was affected by diagenesis in shallow marine environment. Field, petrographical studies in conjunction with REE and stable isotope characteristics suggest that these carbonates form part of the ophiolitic mélange zone that emplaced during subduction and obduction processes of the Indian plate and Myanmar plate collision.

Acknowledgments We are also thankful to the Director, Wadia Institute of Himalayan Geology (WIHG), Dehradun for providing necessary facilities. The work is partially supported by the DST under SERC-Fast Track Project (No. SR/FTP/ES-145/2010) to the first author (AKS). Special thanks are extended to the anonymous reviewers for their valuable comments that improved the manuscript.

References

Acharyya SK (2007) Collisional emplacement history of the Naga-Andaman ophiolites and the position of the eastern Indian suture. J Asian Earth Sci 29:229–242

Acharyya SK, Roy DK, Mitra ND (1986) Stratigraphy and palaeontology of the Naga Hills ophiolite belt. Mem Geol Surv India 119:64–79

Acharyya SK, Ray KK, Roy DK (1989) Tectono-stratigraphy and emplacement history of the ophiolite assemblage from the Naga Hills and Andaman Island arc India. J Geol Soc India 33:4–18

Acharyya SK, Ray KK, Sengupta S (1990) Tectonics of the ophiolite belt from Naga Hills and Andaman Islands, India. Proc India Acad Sci (Earth Planet Sci) 99(2):187–199

Agrawal OP, Ghose NC (1986) Geology and stratigraphy of the Naga Hills ophiolite between Meluri and Awangkhoo–Phek district, Nagaland, India. In: Ghose NC, Varadarajan S (eds) Ophiolites and Indian plate margin. Sumna Publication, Patna, pp 163–195

Allan JR, Matthews RK (1977) Carbon and oxygen isotopes as diagenetic and stratigraphic tools: data from surface and subsurface of Barbados, West Indies. Geology 5:16–20

Armstrong-Altrin JS, Verma SP, Madhavaraju J, Lee YI, Ramasamy S (2003) Geochemistry of Late Miocene Kudankulam Limestones, South India. Int Geol Rev 45:16–26

Armstrong-Altrin JS, Lee YI, Verma SP, Worden RH (2009) Carbon, oxygen, and strontium isotope geochemistry of carbonate rocks of the Upper Miocene Kudankulam formation, Southern India: implications for paleoenvironment and diagenesis. Chemie der Erde Geochem 69:45–60

Armstrong-Altrin JS, Madhavaraju J, Sial AN, Kasper-Zubillaga JJ, Nagarajan R, Flores-Castro K, Rodrigues JL (2011) Petrography and stable isotope geochemistry of the Cretaceous EI Abra Limestones (Actopan), Mexico: implication on diagenesis. J Geol Soc India 77:349–359

Bau M, Dulski P (1996) Anthropogenic origin of positive gadolinium anomalies in river waters. Earth Planet Sci Lett 143:245–255

Baxter AT, Aitchison JC, Zyabrev SV, Ali JR (2011) Upper Jurassic radiolarians from the Naga ophiolite, Nagaland, northeast India. Gond Res 20:638–644

Bellanca A, Masetti D, Neri R (1997) Rare earth elements in limestone/marlstone couplets from the Albian–Cenomanian Cismon section (Venetian region, northern Italy): assessing REE sensitivity to environmental changes. Chem Geol 141:141–152

Bhattacharjee CC (1991) The ophiolites of northeast India: a subduction zone ophiolite complex of the Indo-Burman orogenic belt. Tectonophysics 191:213–222

Bowman JR (1998) Stable-isotope systematics of skarn. In: Lentz DR (ed) Mineralized intrusion-related Skarn systems, mineralogical association of Canada, Calgary, Short Course, vol 26, pp 99–145

Brand U, Veizer J (1980) Chemical diagenesis of a multicomponent carbonate system. 1. Trace element. J Sediment Res 50:1219–1236

Brunnschweiler RO (1966) In the geology of Indo Burman Range. J Geol Soc Austr 13:137–195

Buonocunto FP, Sprovieri M, Bellanca A, D'argenio B, Ferreri V, Neri R, Ferruzza G (2002) Cyclostratigraphy and high-frequency carbon isotope fluctuations in Upper Cretaceous shallow-water carbonates, southern Italy. Sedimentology 49:1321–1337

Chatterjee N, Ghose NC (2009) Metamorphic evolution of the Naga Hills eclogites and blueschist, Northeast India: implications for early subduction of the Indian plate under the Burma microplate. J Metamorph Geol 28:209–225

Chattopadhyay BM, Venkataraman P, Roy DK, Ghose S, Bhattacharya S (1983) Geology of Naga Hills ophiolites. Rec Geol Surv India 113:59–115

Chungkham P, Jafar SA (1998) Late Ctretaceous (Santonian–Maastrichtian) integrated Coccolith-Globotruncanid biostratigraphy of pelagic limestone from the accretionary prism of Manipur, Northeastern India. Micropaleontology 44:68–83

Chungkham P, Mishra PK, Sahni A (1992) Late and terminal Cretaceous foraminifera assemblages from Ukhrul mélange zone, Manipur. Curr Sci 62(6):478–481

Danielson A, Moller P, Dulski P (1992) The europium anomalies in banded iron formations and the thermal history of the oceanic-crust. Chem Geol 97:89–100

De Baar HJW, German CR, Elderfield H, Van Gaans P (1988) Rare earth element distributions in anoxic waters of the Cariaco Trench. Geochim Cosmochim Acta 52:1203–1219

Derry LA, Jacobsen SB (1990) The chemical evolution of Precambrian seawater: evidence from REEs in banded iron formations. Geochim Cosmochim Acta 54:2965–2977

Dilek Y, Furnes H (2009) Structure and geochemistry of Tethyan ophiolites and their petrogenesis in subduction rollback systems. Lithos 113:1–20

Douville E, Bienvenu P, Charlou JL, Donval JP, Fouquet Y, Appriou P, Gamo T (1999) Yttrium and rare earth elements in fluids from various deep-sea hydrothermal systems. Geochim Cosmochim Acta 63:627–643

Elderfield H (1988) The oceanic chemistry of the rare-earth elements. Philos Trans Royal Soc London 325:105–126

Elderfield H, Pagett R (1986) Rare earth elements in icthyoliths: variations with redox conditions and depositional environments. Sci Total Environ 49:175–197

Folk RL (1962) Spectral subdivision of limestone types. In: Ham WE (ed) Classification of carbonate rocks. Am Assoc Petrol Geol Mem 1:62–84

Friedman I, O'Neil JR (1977) Compilation of stable isotope fractionation factors of geochemical interest. In: Fleischer M (ed) Data of geochemistry, 6th edn. US Geol Surv Professional Paper 440-KK, p 12

Frimmel HE (2009) Trace element distribution in Neoproterozoic carbonates as palaeoenvironmental indicator. Chem Geol 258:338–353

Gansser A (1980) The significance of the Himalayan suture zone. In: Tater JM (ed) The alpine Himalayan Region, Tectonophysics 62:37–52

Geological Survey of India (1987) Geological map of Manipur, M.N.C. DRG. No. 42/87

German CR, Elderfield H (1989) Rare earth elements in Saanich Inlet, British Columbia, a seasonally anoxic basin. Geochim Cosmochim Acta 53:2561–2571

German CR, Elderfield H (1990) Application of the Ce anomaly as a paleoredox indicator: the ground rules. Paleoceanography 5:823–833

German CR, Higgs NC, Thomson J, Mills R, Elderfield H, Blusztajn J, Fleer AP, Bacon AP (1993) A geochemical study of metalliferous sediment from the TAG hydrothermal mound, 26°08′N, Mid-Atlantic Ridge. J Geophys Res 98:9683–9692

German CR, Hergt J, Palmer MR, Edmond JM (1999) Geochemistry of a hydrothermal sediment core from the OBS vent-field, 21°N East Pacific Rise. Chem Geol 155:65–75

Ghose NC, Agrawal, OP, Windley BF (1984) Geochemistry of the blueschist–eclogite association in the ophiolite belt on the Indian plate margin (Abstracts), Patna University, Patna, India, pp 27–30

Ghose NC, Singh RN (1981) Structure of the Naga Hills ophiolites and associated sedimentary rocks in the Tuensang district of Nagaland, N.E. India. Ofioliti 6:237–254

Ghose NC, Agrawal OP, Singh RN (1986) Geochemistry of the ophiolite belt of Nagaland, N.E. India. In: Ghose NC, Varadarajan S (eds) Ophiolite and Indian plate margin. Sumna Publication, Patna, pp 241–293

Ghose NC, Agrawal OP, Chatterjee N (2010) Geological and mineralogical study of eclogite and glaucophane schists in the Naga Hills ophiolite, Northeast India. Island Arc 19:334–356

Hudson JD (1977) Stable isotopes and limestone lithification. J Geol Soc London 133(6):637–660

James NP, Choquette PW (1984) Diagenesis No. 9 Limestones—the meteoric diagenetic environment. Geosci Can 11:161–194

Kato Y, Nakao K, Isozaki Y (2002) Geochemistry of Late Permian Triassic pelagic cherts from southwest Japan: implications for an oceanic redox change. Chem Geol 182:15–34

Keith ML, Weber JN (1964) Carbon and oxygen isotopic composition of selected limestones and fossils. Geochim Cosmochim Acta 28:1787–1816

Kemp RA, Trueman CN (2003) Rare earth elements in Sol nhofen biogenic apatite: geochemical clues to the palaeoenvironment. Sediment Geol 155:109–127

Klinkhammer GP, Elderfield H, Edmond JM, Mitra A (1994) Geochemical implications of rare earth element patterns in hydrothermal fluids from mid-ocean ridges. Geochim Cosmochim Acta 58:5105–5113

Komiya T, Hirata T, Kitajima K, Yamamoto S, Shibuya T, Sawaki Y, Ishikawa T, Shu D, Li Y, Han J (2008) Evolution of the composition of seawater through geologic time, and its influence on the evolution of life. Gond Res 14:159–174

Land LS (1970) Phreatic versus vadose meteoric diagenesis of limestones: evidence from a fossil water table. Sedimentology 14:175–185

Leeder MR (1982) Sedimentology. Chapman and Hall, London, p 344

Madhavaraju J, Lee YI (2009) Geochemistry of the Dalmiapuram formation of the Uttatur group (Early Cretaceous), Cauvery basin, southeastern India: implications on provenance and paleo-redox conditions. Revista Mexicana de Ciencias Geológicas 26:380–394

Madhavaraju J, Ramasamy S (1999) Rare earth elements in limestones of Kallankurichchi formation of Ariyalur Group, Tiruchirapalli Cretaceous, Tamil Nadu. J Geol Soc India 54:291–301

Madhavaraju J, Kolosov I, Buhlak D, Armstrong-Altrin JS, Ramasamy S, Mohan SP (2004) Carbon and oxygen isotopic signatures in Albian–Danian limestones of Cauvery Basin, Southeastern India. Gond Res 7:519–529

Madhavaraju J, González-León CM, Lee YI, Armstrong-Altrin JS, Reyes-Campero LM (2010) Geochemistry of the mural formation (Aptian–Albian) of the Bisbee group, Northern Sonora, Mexico. Cretaceous Res 31:400–414

Mazumdar A, Tanaka K, Takahashi T, Kawabe I (2003) Characteristics of rare earth element abundances in shallow marine continental platform carbonates of Late Neoproterozoic successions from India. Geochem J 37:277–289

Mitchell AHG (1993) Cretaceous–Cenozoic tectonic events in the western Myanmar (Burma) Assam region. J Geol Soc London 150:1089–1102

Mitra ND, Vidyadharan KT, Gour MP, Singh SK, Mishra UK, Khan IK, Ghosh S (1986) A note on the Olitostromal deposits of Manipur. Rec Geol Sur India 114(4):61–76

Murray RW, Buchholtz Brink MR, Brink MR, Gerlach DC, Russ GP III, Jones DL (1991) Rare earth, major and trace elements in chert from the Franciscan complex and Monterey group, California: assessing REE sources to fine grained marine sediments. Geochim Cosmochim Acta 55:1875–1895

Nagarajan R, Madhavaraju J, Armstrong-Altrin JS, Nagendra R (2011) Geochemistry of Neoproterozoic limestones of the Shahabad formation, Bhima Basin, Karnataka, southern India. Geosci J 15(1):9–25

Nath BN, Roelandts I, Sudhakar M, Plueger WL (1992) Rare earth element patterns of the Central Indian Basin sediments related to their lithology. Geophys Res Lett 19:1197–1200

Nath BN, Bau M, Ramalingeswara Rao B, Rao ChM (1997) Trace and rare earth elemental variation in Arabian Sea sediments through a transect across the oxygen minimum zone. Geochim Cosmochim Acta 61:2375–2388

Nelson CS, Smith AM (1996) Stable oxygen and carbon isotope fields for skeletal and diagenetic components in New Zealand Cenozoic non tropical carbonate sediments and limestones: A synthesis and review. N Z J Geol Geophys 39:93–107

Palmer MR (1985) Rare earth elements in foraminifera tests. Earth Planet Sci Lett 73:285–298

Rankamma K (1963) Progress in isotope geology. John Wiley, New York, p 705

Sarkar A, Datta AK, Poddar BC, Bhattacharyya BK, Kollapuri VK, Sanwal R (1996) Geochronological studies of Mesozoic igneous rocks from eastern India. J Southeast Asian Earth Sci 13:77–81

Searle MP, Noble SR, Cottle JM (2007) Tectonic evolution of the Mogok metamorphic belt, Burma (Myanmar) constrained by U-Th-Pb dating of metamorphic and magmatic rocks. Tectonics 26, TC3014. http://dx.doi.org/10.1029/2006TC002083

Sengupta S, Acharyya SK, Vander Hull HJ, Chaltopadhyay B (1989) Geochemistry of volcanic rocks from the Naga Hills ophiolites, northeast India and their inferred tectonic settling. J Geol Soc Lond 146:491–498

Siby K, Nath BN, Ramaswamy V, Naman D, Gnaneshwar Rao T, Kamesh Raju KA, Selvaraj K, Chen CTA (2008) Possible detrital, diagenetic and hydrothermal sources for Holocene sediments of the Andaman backarc basin. Marine Geol 247:178–193

Singh AK (2009) High-Al chromian spinel in ultramafic rocks of Manipur ophiolite Complex, Indo-Myanmar Orogenic Belt: implication for petrogenesis and geo-tectonic setting. Curr Sci 96:973–978

Singh AK (2013) Petrology and geochemistry of Abyssal Peridotites from the Manipur ophiolite Complex, Indo-Myanmar Orogenic Belt, Northeast India: Implication for melt generation in mid-oceanic ridge environment. J Asian Earth Sci 66:258–276

Singh AK, Singh NI, Devi LD, Bikramaditya Singh RK (2012) Geochemistry of Mid-Ocean Ridge Mafic intrusives from the Manipur ophiolitic Complex, Indo-Myanmar Orogenic Belt, NE India. J Geol Soc India 80:231–240

Tewari VC, Sial AN (2007) Neoproterozoic-early Cambrian isotopic variation and chemostratigraphy of the Lesser Himalaya, India, Eastern Gondwana. Chem Geol 237:64–88

Toyoda K, Nakamura Y, Masuda A (1990) Rare earth elements of Pacific pelagic sediments. Geochim Cosmochim Acta 54:1093–1103

Upadhyay R, Sinha AK (1998) Tectonic evolution of Himalayan Tethys and subsequent Indian plate subduction along indus suture zone. PINSA 64(5):659–683

Venkataramana P, Dutta AK, Acharyya SK (1986) Petrography and petrochemistry of Naga Hills ophiolite. Geol Surv India 119:33–63

Vidyadharan KT, Joshi A, Ghose S, Gaur MP, Sukla R (1989) Manipur ophiolites. Its geology, tectonic setting and metallogeny. In: Ghose NC (ed) Phanerozoic ophiolites of India. Sumna Publication, Patna, pp 197–212

Webb GE, Kamber BS (2000) Rare earth elements in Holocene reefal microbialites: a new shallow seawater proxy. Geochim Cosmochim Acta 64:1557–1565

Wright VP (1990) Equatorial aridity and climatic oscillations during the Carboniferous, Southern Britain. J Geol Soc Lond 147:359–363

Zhao YY, Zheng YF, Chen F (2009) Trace element and strontium isotope constraints on sedimentary environment of Ediacaran carbonates in southern Anhui, South China. Chem Geol 265:345–362